Journal of the European Ceramic Society 20 (2000) 227–233

# Microstructure and mechanical properties of in situ produced $SiC/TiSi_2$ nanocomposites

Jianlin Li*, Dongliang Jiang, Shouhong Tan

*State Key Lab of High Performance Ceramics and Superfine Microstructure, Shanghai Institute of Ceramics, Chinese Academy of Sciences, 1295 Dingxi Road, Shanghai 200050, China*

Received 15 February 1999; received in revised form 29 March 1999; accepted 11 May 1999

**Abstract**

The microstructure and mechanical properties of in situ produced $SiC/TiSi_2$ nanocomposites have been studied. The results indicate that $SiC/TiSi_2$ composites can be fabricated by reactively hot pressing mixed powders of TiC, elemental Si and elemental Ti. The in situ produced SiC particles are close to nanosize. Without elemental Ti powder, the composite obtained consists of $TiSi_2$ 66 vol% and SiC 34 vol% without residual Si or TiC. At ambient temperature, the highest bending strength of $SiC/TiSi_2$ composites was 400 MPa, twice that of monolithic $TiSi_2$. Also fracture toughness of $SiC/TiSi_2$ composites exceeds that of pure $TiSi_2$. At 1200°C, the yield strength of composites was improved due to the presence of the SiC particles. 

*Keywords:* Mechanical properties; Microstructure; Nanocomposites; SiC; $TiSi_2$

## 1. Introduction

Intermetallic compounds with low density and improved oxidation resistance are being considered for a wide range of high temperature applications and much research effort has been devoted to their development in the last ten years. For structural applications in harsh environments, a material should have adequate strength, creep resistance, and oxidation resistance. Silicides might be especially well suited for such applications due to the potential for good oxidation resistance at high temperatures. But the problems of fracture and poor toughness at ambient temperature and poor creep behavior at elevated temperature remain. In order to overcome these difficulties, a wide knowledge of silicides and related compounds is necessary.[1–9]

Titanium silicides are very attractive for applied temperatures up to 1300°C and higher. $TiSi_2$ exhibits low density, high temperature strength and excellent oxidation resistance. In addition, the thermal and electrical conductivities are relatively high, making the material attractive for electronic interconnection and diffusion barriers.

$TiSi_2$ compound is a face centred ordered orthorhombic C54 type of structure with the lattice constants $a=0.8275$, $b=0.4799$, $c=0.8547$ nm, and with a density of 4070 kg $m^{-3}$. The congruent melting temperature is 1540°C.

Monolithic $TiSi_2$ has been successfully fabricated by Rosenkranz.[10] The intermetallic compound was synthesized by reaction sintering in vacuum in the temperature range from 1400 to 1500°C. The conglomerates obtained were ground in argon atmosphere to powder, then compacted by the hot isostatic pressing technique.[10]

However, monolithic $TiSi_2$ material is very brittle and its high temperature strength is also unsatisfactory. A promising alternative method is to produce a $TiSi_2$ matrix composite. SiC is compatible with $TiSi_2$; however, the thermal expansion coefficient difference ($4.8\times10^{-6}$/°C for SiC, $9\times10^{-6}$/°C for $TiSi_2$) might lead to microcrack formation if large SiC particles are incorporated. In this paper, the microstructure and mechanical properties of in situ produced $SiC/TiSi_2$ nanocomposites prepared by hot pressing mixed powders of TiC, Ti and Si have been studied.

* Corresponding author.

0955-2219/00/$ - see front matter 
PII: S0955-2219(99)00157-0

## 2. Experimental

The mixed powder of TiC, Ti and Si, with composition chosen to yield SiC volume from 8 to 34 vol% in the product, was wet blended for 5 h with SiC media. After drying, the mixed powder was blended for another 5 h with SiC media. $SiC/TiSi_2$ samples were fabricated by reactively hot pressing the mixed powder at 35 MPa and 1380°C for 1 h in Ar. The heating rate was 15°C $min^{-1}$. In order to compare the mechanical properties of monolithic $TiSi_2$ material with that of $SiC/TiSi_2$, mixed powder of Ti and Si was used to produce $TiSi_2$ via the same process.

The density of samples was obtained by the Archimedes' method using pure water at room temperature.

When the samples were metallographically polished, X-ray diffraction (XRD) was carried out to identify the phases present. Microstructural characterization was carried out using scanning electron microscopy (SEM). The grain size of the matrix was obtained by quantitative analysis of polished surfaces etched in acid solution ($HF:HNO_3:H_2O$, 1:1:1) for 5 s. Submicrostructural characterization has been carried out using transmission electron microscopy (TEM) and EDAX analysis. TEM samples were studied using a JEM-200cx operating at 200 kv.

Rectangular bars, $3\times4\times36$ $mm^3$, were prepared for bending tests. Using a universal testing machine (Instron 1185) with a span of 30 mm. Experiments were conducted at 20°C and 1200°C in air. The speed of crosshead displacement was 0.5 mm $min^{-1}$. Indentation was employed to determine the fracture toughness $K_{IC}$ at room temperature using a Vickers' diamond indentor. $K_{IC}$ was calculated by the following formula:

$$K_{IC} = P(\pi c)^{-3/2}\cot\beta$$

where $2C$ is the length of crack. Load $P = 10^4$ g, and $\beta = 68°$.

## 3. Results and discussion

### 3.1. Microstructure

Fig. 1 shows the XRD patterns of, (a) $SiC/TiSi_2$ composite, and (b) $TiSi_2$. The results confirm that $TiSi_2$ and $SiC/TiSi_2$ composite can be produced via reactive hot pressing. The reactions taking place are,

$$3Si + TiC = SiC + TiSi_2 \quad (1)$$

$$2Si + Ti = TiSi_2 \quad (2)$$

The Gibbs free energy change of reactions [Eqs. (1) or (2)] is negative, the heat evolved in the exothermic reaction [Eq. (1)] being 23.4 kJ $mol^{-1}$ and 97.4 kJ $mol^{-1}$ in reaction [Eq. (2)]. [11]

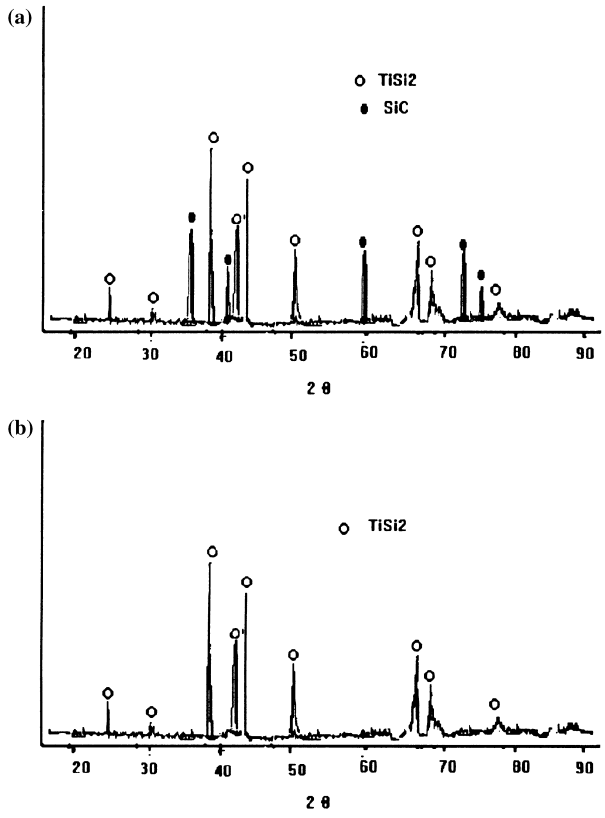


Fig. 1. XRD patterns of (a) $SiC/TiSi_2$ composite with 34 vol% β-SiC, (b) $TiSi_2$.

$SiC/TiSi_2$ composite with 34 vol% SiC was fabricated by hot pressing the stoichiometric mixed powder of TiC and Si according to reaction [Eq. (1)]. Pure $TiSi_2$ material was obtained by reaction [Eq. (2)]. Other composites involve both reaction [Eqs. (1) and (2)]. The SiC is compatible with the $TiSi_2$ matrix.

Fig. 2(a) shows the microstructure of $34SiC/TiSi_2$ composite under an optical microscope. Fig. 2(b) and (c) were backscattered SEM micrograph of $34SiC/TiSi_2$ and $18SiC/TiSi_2$ composites, respectively. The dark phase is SiC and bright $TiSi_2$. Few pores were found because the hot pressing temperature (1380°C) was high enough compared with $TiSi_2$ melting point (1540°C). The phase boundary of SiC and $TiSi_2$ was indistinct. The dark spots in Fig. 2(a) were clusters of fine SiC grains rather than single SiC crystals. These clusters were about 15 μm in size.

Table 2 gives the $TiSi_2$ grain size and relative density of the composites calculated using the identified composites.

### 3.2. Submicrostructure and reaction mechanism

In order to study the submicrostructure of the $SiC/TiSi_2$ composites, TEM analyses were carried out. Fig. 3(a)

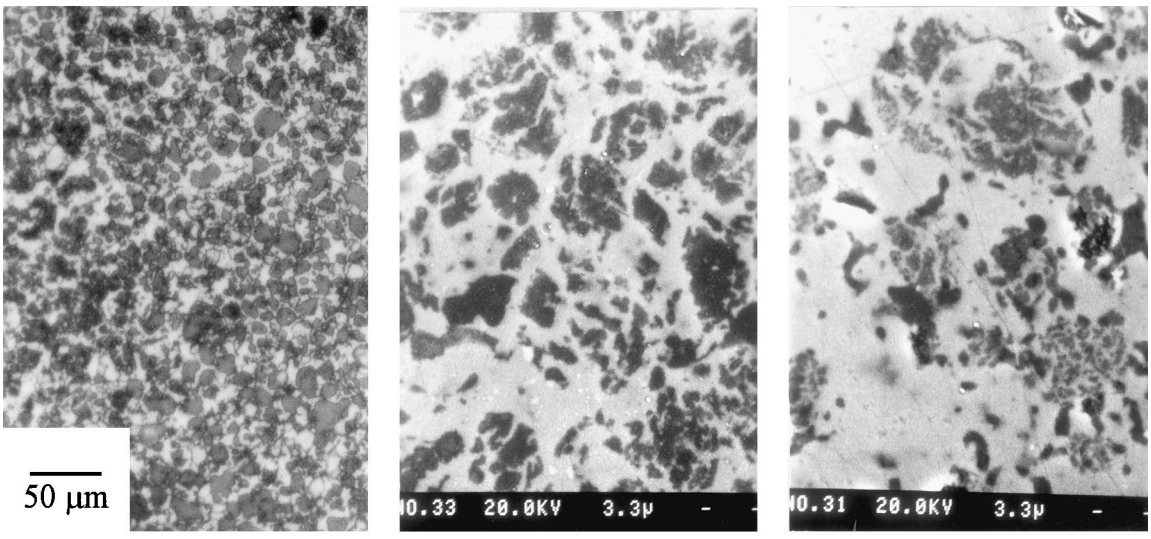


Fig. 2. Optical micrograph of 34SiC/$TiSi_2$ composite (a), backscattered SEM micrograph of 34SiC/$TiSi_2$ composite fabricated through reaction Eq. (1) (b), 18SiC/$TiSi_2$ composites fabricated through reactions [Eqs. (1) and (2)] (c).

Table 1
Characteristics of powder used in this work

| Powder | Purity (%) | Particle characteristics |
|---|---|---|
| Ti | 99·5 | −300 mesh |
| Si | 99·5 | −300 mesh |
| TiC | 99·0 | 3·5 μm |

Table 2
$TiSi_2$ grain size and relative density of composites

| SiC content (vol %) | 0 | 8 | 18 | 34 |
|---|---|---|---|---|
| $TiSi_2$ grain size (μm) | 20 | 15 | 8 | 3 |
| Relative density (%) | 98 | 99 | 98 | 99 |

shows that there were many SiC particles associated with a single $TiSi_2$ grain, suggesting that SiC particles were not well distributed in the matrix. In situ produced SiC grains were no more than 300 nm in size. Fig. 3(a) also shows some nanosized SiC grains in a $TiSi_2$ grain.

Fig. 3(b) shows a magnified SiC grain, nearly 350 nm long and 200 nm wide. It can be seen that the SiC particle was faulted.

Fig. 4 gives the HRTEM image of the grain boundary of SiC and $TiSi_2$. There was no amorphous phase on the grain boundary. An amorphous phase, such as $SiO_2$, is known to damage the $TiSi_2$ material mechanical properties, causing a decrease in $K_{IC}$ from 500 to 700°C.[10] Usually, it has been difficult in powder hot pressing to fabricate composites without grain boundary phase, because the original powder has often been wrapped in an oxidation layer. The HRTEM image in Fig. 4 shows that the SiC particle has the $\beta$ structural lattice, consistent with the result of XRD.

In the hot pressing process, the Si and Ti particles (−300 mesh) were much larger than those of TiC, therefore, TiC particles tended to be spaced among the Si and Ti particles. If the Si and Ti particles can be ordered as spheres, the spacing between the Si and Ti particles would be nearly 20 m; this would be reduced because of the pressure.

At the hot pressing temperature, Si, now soft, will react with TiC. In this process, TiC decomposes while Ti atoms and C atoms diffuse into the Si phase. In view of the reactions all being exothermic reactions, the Si particles are expected to undergo partial melting. Therefore, Si was continuously pushed against the TiC particles because of the pressure. If the diffusing of C is relatively slow, SiC grains, with some $TiSi_2$ grains, form clusters where the TiC particles were gathered before reaction. Since the TiC particles were enveloped by the Si phase, many SiC grains simultaneously formed near the surface of the TiC particles. Considering that the TiC particles were just 3.5 μm in size, the in situ produced SiC grains were also fine. In the hot pressing process, some neighboring fine SiC grains were sintered into agglomerates. On the other hand, the $TiSi_2$ grains on the edge of clusters, not as much affected by the SiC particles as those $TiSi_2$ grains co-existing with SiC in clusters, grew into large grains. As a result, the microstructure in Fig. 2 was created.

Fig. 2 shows that the dark phase, namely the clusters formed of SiC grains and $TiSi_2$ grains, were nearly 15 m in size. This result is consistent with the size of the intervals (20 μm) between Si and Ti particles. Fig. 5 is a diagram of the reaction.

As discussed, the TiC particles formed agglomerates between the Ti and Si particles before the reaction

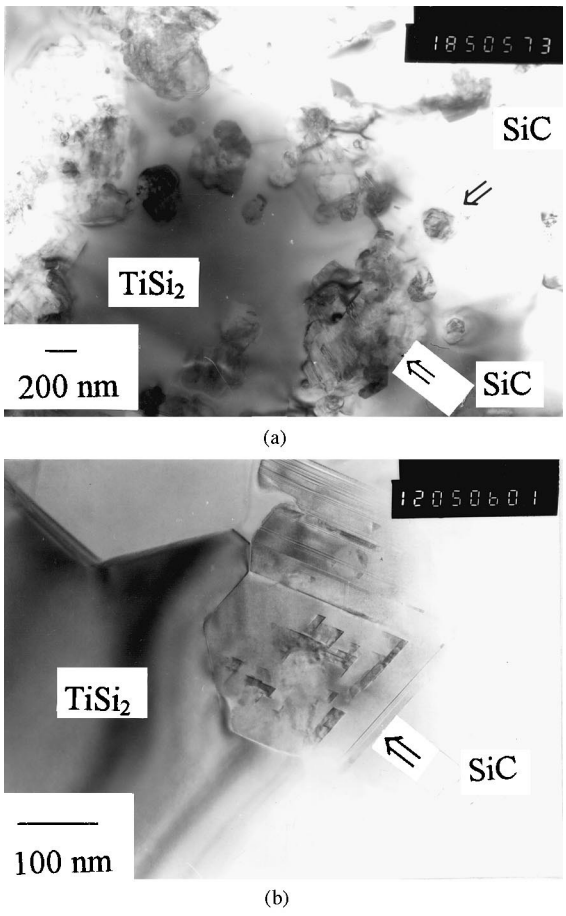


Fig. 3. TEM images of, (a) fine SiC grains and some SiC agglonerates formed from fine SiC grains, and some fine SiC grains in a $TiSi_2$ grain, (b) a magnified SiC grain.

which led to the clusters of SiC, therefore, a finer microstructure could be obtained and SiC agglomerates could be avoided if finer Ti and Si powder were used.

### 3.3. Mechanical properties at ambient temperature

The bending strength reached 400 MPa, more than twice that of monolithic $TiSi_2$. Fig. 6 shows the dependence of bending strength on SiC content. $SiC/TiSi_2$ composites achieved higher strength with higher SiC content. Another factor relating to strength was the $TiSi_2$ matrix grain size (Table 2 shows the grain size of composites). The nanosized SiC particles restrained the growth of $TiSi_2$ grains and decreased abnormal grain growth.[12] Finer grains are commonly associated with higher strength.

Fig. 7(a) is an SEM micrograph of the fractured surface of pure $TiSi_2$. The fracture surface was smooth. The $TiSi_2$ grains were coarse and fracture was fully transgranular. Fig. 7(b) shows $34SiC/TiSi_2$. It can be observed that the $TiSi_2$ grains in this material were finer than in pure $TiSi_2$ and the fractured surface was rather rough. Short strings of fine grains can be seen on the fracture surface.

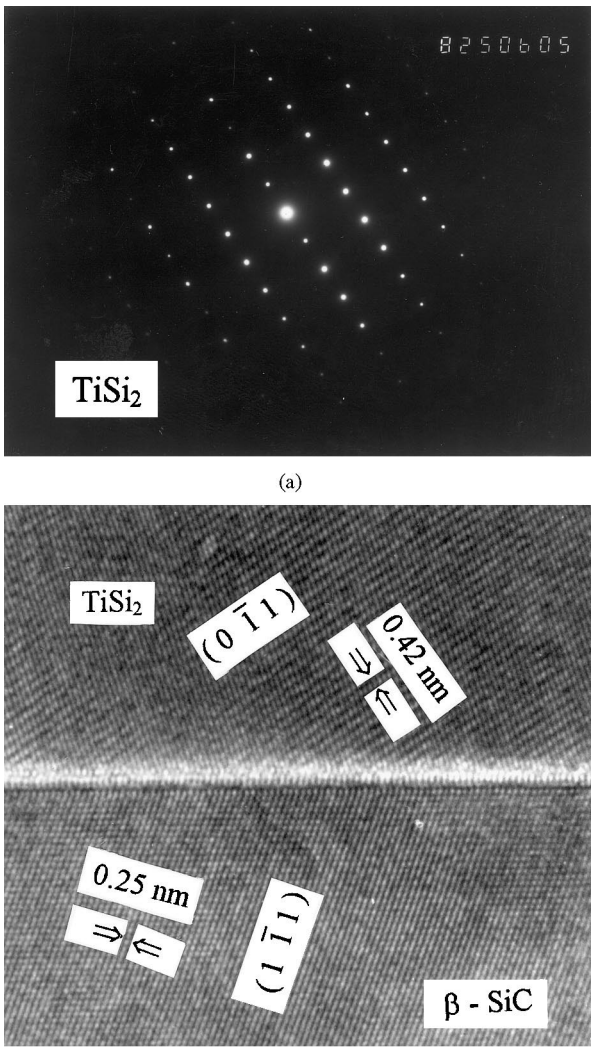


Fig. 4. HREM image of the grain boundary of SiC and $TiSi_2$.

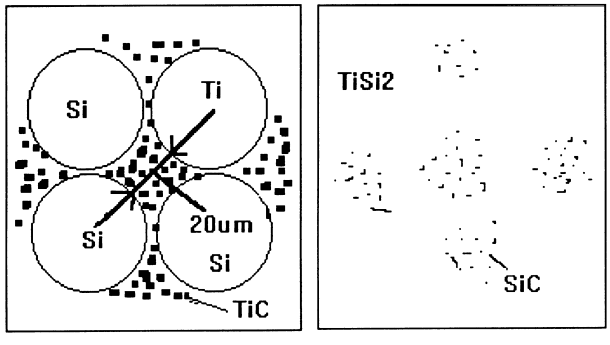


Fig. 5. Sketch of reaction between Ti, Si and TiC. Before reaction, fine TiC particles are separated by nearly 20 μm and are pushed together during hot pressing. After reaction, SiC grains occur at these sites.

The fracture toughness of composites is shown in Fig. 8. Compared with the much improved strength of composites, the toughness of the composites was also slightly improved.

SiC grains in the $TiSi_2$ matrix induce residual stress due to the thermal expansion coefficient dismatch. However, in view of the fine size of the SiC grains, the distance of residual stress is short and there is little ability to affect the extension of a crack. Stress striations were observed around SiC agglomerates, but few were found near single SiC grains. Fig. 9 shows the stress in a $TiSi_2$ grain induced by a SiC agglomerate on a triple grain boundary.

Fig. 10 shows the trajectory of an indentation crack extension. The slight increment of toughness is in part attributable to crack deflection caused by residual stress.

### 3.4. Strength at elevated temperature

$TiSi_2$ exhibits a brittle to ductile transition at 805°C. At higher temperature, the strength of $TiSi_2$ decreases sharply due to thermally activated dislocations.[10] Fig. 11 shows the dependence of the yield strength (0.2% offset) of the composites on the SiC content.

$SiC/TiSi_2$ composites show much higher yield strength than pure $TiSi_2$. Fine SiC particles, in the $TiSi_2$ grains or on the grain boundary, act as barriers to gliding dislocations and distortion of the $TiSi_2$ grains. Furthermore, the absence of amorphous phase at the grain boundary between SiC and $TiSi_2$ is helpful to high temperature strength.

Fig. 12 illustrates the relation between stress and displacement for $18SiC/TiSi_2$. Yield occurs at 80 MPa. During the plastic deforming, there is no obvious work hardening effect.

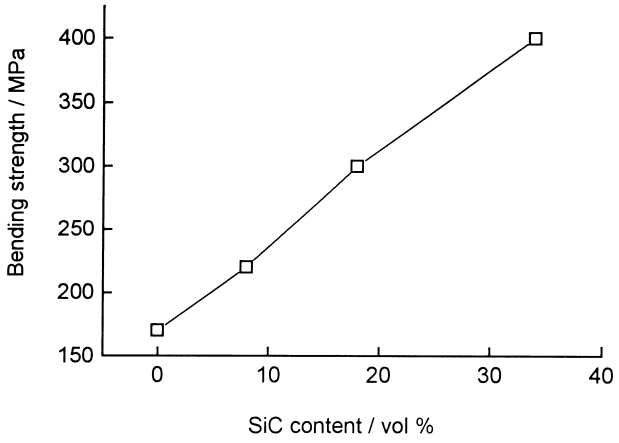


Fig. 6. Dependence of bending strength of $SiC/TiSi_2$ composites on SiC content.

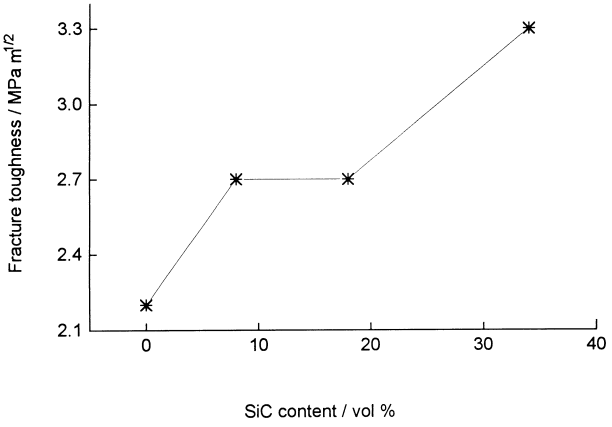


Fig. 8. Fracture toughness of composites as a function of SiC content.

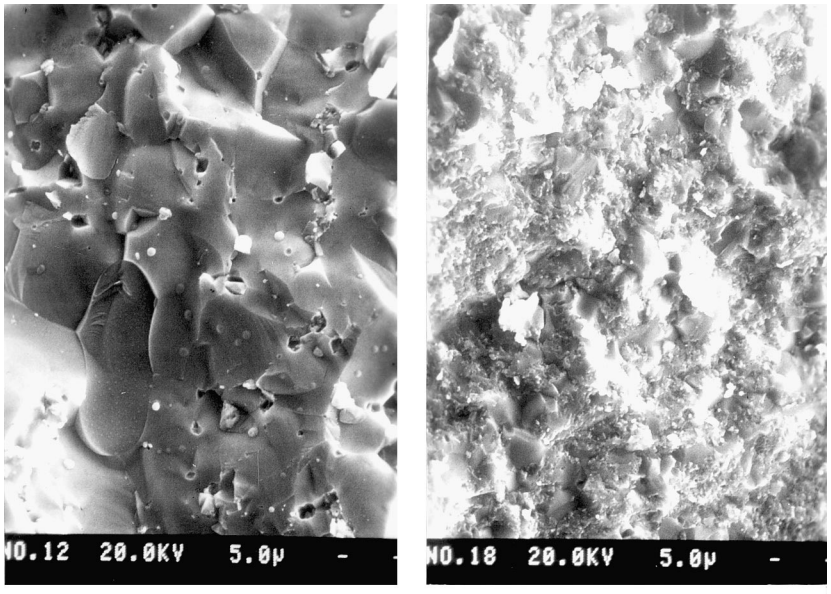


(a) (b)

Fig. 7. SEM micrographs of fractured surface of (a) pure $TiSi_2$, (b) $34SiC/TiSi_2$ composite.

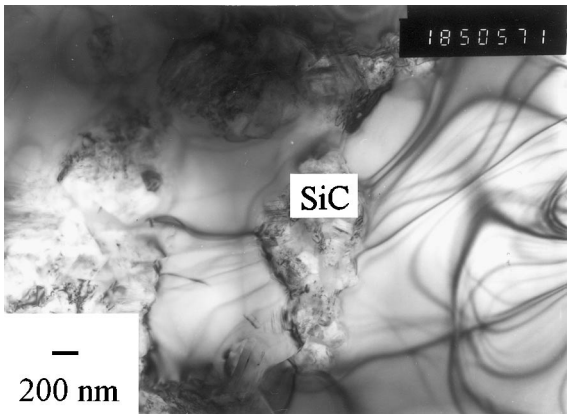


Fig. 9. Stress striations indicative of residual stress at a $TiSi_2$ grain.

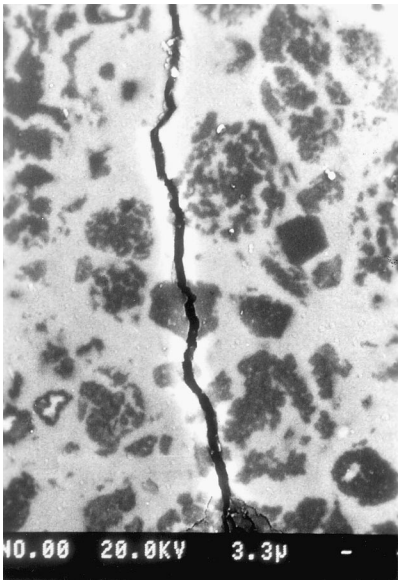


Fig. 10. Indentation crack extension in 34 $SiC/TiSi_2$ composite.

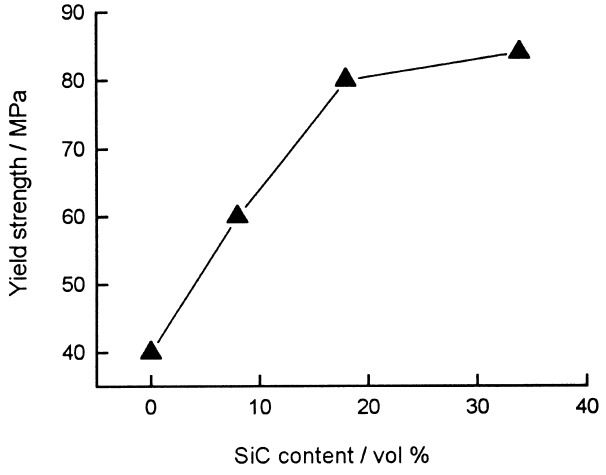


Fig. 11. Dependence of yield strength of $SiC/TiSi_2$ composites on SiC content at 1200°C.

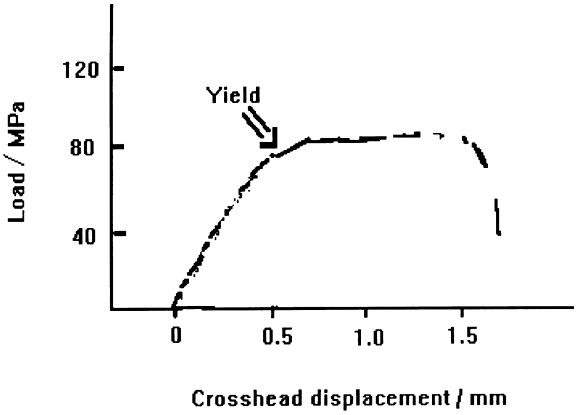


Fig. 12. Load and crosshead displacement for 18 $SiC/TiSi_2$ at 1200°C.

## 4. Conclusion

$SiC/TiSi_2$ nanocomposites can be produced by reactively hot pressing mixed powders of TiC, elemental Si and Ti. In situ produced SiC particles are fine with some of them in the $TiSi_2$ grains. There was no amorphous phase at the grain boundary of SiC and $TiSi_2$. At ambient temperature, the highest bending strength of $SiC/TiSi_2$ composite was 400 MPa, twice that of monolithic $TiSi_2$. The fracture toughness of the composite also exceeds that of pure $TiSi_2$. At elevated temperature (1200°C), the highest yield strength of $SiC/TiSi_2$ composites was twice that of pure $TiSi_2$.

## References

1. Vasudeevan, A. K., A comparative overview of molybdenum disilicide composites. *Mat. Sci. Eng.*, 1992, **A155**, 1–17.
2. Shaw, L., Control of the interfacial reactions in Nb-toughened $MoSi_2$. *J. Am. Ceram. Soc.*, 1993, **76**(9), 2305–2311.
3. Shah, D. M., Appraisal of other silisides as structural materials. *Mat. Sci. Eng.*, 1992, **A155**, 45–57.
4. Ward, C. M., Intermetallic matrix composites a review. *Intermetallics*, 1996, **4**, 217–229.
5. Mitra, R., Processing microstructure property relationship in reaction hot pressed and composites. *Mat. Sci. Eng.*, 1997, **A225**, 15–17.
6. Lee, J. I., *In situ* processing and properties of $SiC/MoSi_2$ nanocomposites. *J. Am. Ceram. Soc.*, 1998, **81**(2), 421–424.
7. Aikin, R. M., Structure and properties of *in situ* reinforced $MoSi_2$. *Ceram. Eng. Sci. Proc.*, 1991, **12**(9–10), 1643–1652.
8. Shah, D. M., Evaluation of refractory intermetallics with A15 structure for high temperature structural applications. *Mat. Sci. Eng.*, 1992, **A153**, 402–407.
9. Petrovic, J. J., $ZrO_2$-reinforced $MoSi_2$ matrix composite. *Ceram. Eng. Sci. Proc.*, 1991, **12**(9–10), 1633.
10. Rosenkranz, R., Microstructures and properties of high

melting point intermetallics $Ti_5Si_3$ and $TiSi_2$ composites. *Mat. Sci. Eng.*, 1992, **A152**, 288–294.
11. Barin, I., Knacke, O., *Thermochemical Properties of Inorganic Substances*. Springer Verlag, Berlin, Heidelberg, New York, 1973, pp. 674, 749, 754, 790.
12. Nihara, K., New design concept of structural ceramics—ceramic nanocomposites. *J. Ceram. Soc. Jpn*, 1991, **99**(10), 974–982.